In memory of Professor Gérard A Maugin

MMS

Mathematics and Mechanics of Solids
2020, Vol. 25(7) 1405–1415

DOI: 10.1177/1081286517713243
journals.sagepub.com/home/mms
SAGE

Dimensioning of thick-walled spherical and cylindrical pressure vessels

Patrick Schneider
Institute for Lightweight Construction and Design (KLuB), Department of Mechanical Engineering, Technische Universität Darmstadt, Darmstadt, Germany

Reinhold Kienzler
*Bremen Institute for Mechanical Engineering (bi**me**), Department of Production Engineering, University of Bremen, Bremen, Germany*

Received 15 March 2017; accepted 10 May 2017

Abstract
In this contribution, we revisit the rather classical problem of Lamé and provide a novel and easy way to plot the stress distributions and the overall absolute maximum von Mises stress for arbitrary parameters in only two diagrams. We also provide a maximum hoop stress formula for combined loading and an extensive discussion covering the accuracy of dimensioning via the maximum hoop stress instead of the maximum von Mises stress, as well as the accuracy of the classical approximative hoop stress formulas.

Keywords
Dimensioning, pressure vessels, thick-walled, thin-walled, linear elasticity, Lamé's problem, exact solution, hoop stress formula, through-thickness stress distribution, von Mises stress

1. Introduction

The honoree of this special issue contributed a lot to the field of teaching mechanics and we are sure that he would agree that often enough the simplest examples are the ones from which one can learn the most. Also, often enough, there is still a lot left to discover even for basic examples which are part of every introductory text book. In this spirit, we revisit the very classical example of a linear elastic thick-walled pressure vessel, which is one of the rare examples of a three-dimensional problem of linear elasticity that has an easy to derive exact, analytical solution and is therefore of utmost value for courses in strength-of-materials or elasticity.

The solution of this problem goes way back to the work by Lamé [1] and hence the problem itself is often referred to as *Lamé's problem*. The simple approximations of the hoop stresses for thin walled spherical and cylindrical vessels

$$\sigma_{\varphi\varphi}^{\text{sph.}} = \sigma_{\vartheta\vartheta} = \frac{p_i r_i}{2t}, \quad \sigma_{\varphi\varphi}^{\text{cyl.}} = \frac{p_i r_i}{t} \tag{1}$$

Corresponding author:
Patrick Schneider, Institute for Lightweight Construction and Design (KLuB), Department of Mechanical Engineering, Technische Universität Darmstadt, Otto-Berndt-Straße 2, D-64287 Darmstadt, Germany.
Email: patrick.schneider@klub.tu-darmstadt.de

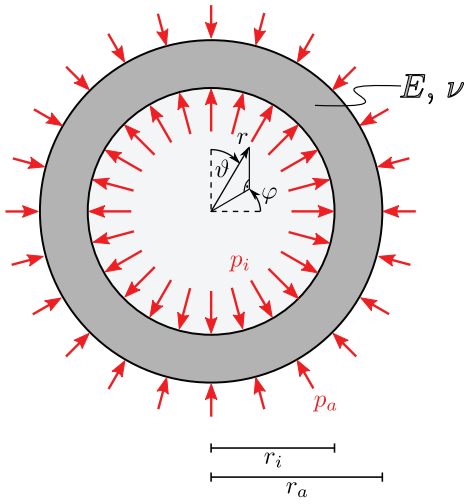

Figure 1. Thick-walled sphere loaded by inner p_i and outer pressure p_a.

are even older. First experimental investigations date back to circa 1670, cf. [2]. Nowadays the formulas are part of nearly every basic course text book on mechanics of materials, since their relevance for the design of pressure vessels remains. While some books cover only the classical formulas, like e.g. [3–8], others treat Lamé's problem as well, like e.g. [9–21]. Particular detailed investigations of Lamé's problem are given by Budynas and Stark [10, 19]. The most detailed investigation we found in the book by Läpple [16], which is only available in German. Also, there are still present papers dealing with the problem. A recent review about simple analytical formulas for hoop stresses in pressure vessels can be found in Sinclair and Helms [2]. However, the majority of newer papers treat extensions of Lamé's problem towards more complex material models, like elastoplastic material and strain gradient theories, cf. [22–24], materials undergoing creep and creep damage, cf. [25, 26] and the most recent series of papers treats functionally graded materials, cf. [27–30].

Most books dealing with Lamé's problem only derive the formulas but give no graphical interpretation of the results. The books that do so, like e.g. [10, 16, 1 9], print sample distributions for the stresses for parameters which were chosen at random. In this contribution we present an easy way to plot the stress distributions of the problem for arbitrary parameters in only two diagrams using a dimensionless formulation and a (to our best knowledge) yet undiscovered simple mathematical relation between the inner- and outer-pressure solution, cf. equations (13) and (21). The diagrams allow for a graphical determination of the stress state in arbitrary points of the vessel and the overall maximum von Mises stress as well.

We also provide a maximum hoop stress formula for combined loading and an extensive discussion covering the topics of the accuracy of dimensioning via the maximum hoop stress instead of the maximum von Mises stress, as well as the accuracy of the classical approximative hoop stress formulas.

2. The exact solution for the thick-walled spherical vessel

First, we seek the displacement-field $u = (u_i)$ of a thick-walled spherical vessel loaded by inner p_i and outer pressure p_a and the associated stress-field $\sigma = (\sigma_{ij})$. For convenience, the problem is formulated using a spherical coordinate system which is originated in the center of the vessel. The inner radius of the vessel is denoted by r_i and the outer radius is denoted by r_a, where $0 < r_i < r_a$. The material of the vessel is assumed to be homogeneous, linear elastic. In order to render the strain energy positive definite, the modulus of elasticity must be positive, $E > 0$, and Poisson's ratio must lie in the range $-1 < \nu < 0.5$. Most engineering materials exhibit a positive value of ν. Materials with negative Poisson's ratio are called auxetic materials and are usually only treated by special literature, c.f. e.g. [31]. However, all considerations in this contribution apply for auxetic materials as well. The shear modulus is denoted by G. The problem is sketched in Figure 1.

Due to the spherical symmetry of geometry and loading, the displacements (beside rigid body motions) can only take place in radial direction and can only depend on the radial coordinate

$$u_r = u_r(r),\ u_\varphi = 0,\ u_\vartheta = 0. \tag{2}$$

Therefore, the linearized strain tensor $\varepsilon = \varepsilon_{ij}$ has the simple representation [32]

$$\varepsilon_{ij} = \begin{pmatrix} u_{r,r} & 0 & 0 \\ 0 & \frac{u_r}{r} & 0 \\ 0 & 0 & \frac{u_r}{r} \end{pmatrix} \tag{3}$$

and the spherical coordinate system turns out to coincide with the principal axes. By insertion into Hook's law the non-vanishing stress components can be derived as

$$\sigma_{rr} = \frac{E}{(1+\nu)(1-2\nu)} \cdot \left((1-\nu)\, u_{r,r} + 2\nu\, \frac{u_r}{r} \right) , \tag{4}$$

$$\sigma_{\varphi\varphi} = \sigma_{\vartheta\vartheta} = \frac{E}{(1+\nu)(1-2\nu)} \cdot \left(\nu\, u_{r,r} + \frac{u_r}{r} \right), \tag{5}$$

whereas

$$\sigma_{r\varphi} = \sigma_{\varphi\vartheta} = \sigma_{\vartheta r} = 0,$$

Because of the simple structure of the stress tensor, it is easy to see that two of the three equilibrium equations are fulfilled identically. Only the equation in the radial direction has to be considered, which simplifies to

$$\sigma_{rr,r} + \frac{1}{r} \left(2\sigma_{rr} - \sigma_{\vartheta\vartheta} - \sigma_{\phi\phi} \right) = 0. \tag{6}$$

Insertion of the stresses given by equations (4) and (5) into the remaining equilibrium equation (6) leads to the ordinary differential equation

$$\begin{aligned} &\sigma_{rr,r} + \frac{1}{r} \left(2\sigma_{rr} - \sigma_{\vartheta\vartheta} - \sigma_{\phi\phi} \right) \\ &= \frac{E\,(1-\nu)}{(1+\nu)(1-2\nu)} \left[u_{r,rr} + \frac{2}{r} u_{r,r} - \frac{2}{r^2} u_r \right] = 0 \\ \Leftrightarrow &\left[\frac{1}{r^2} \left(r^2\, u_r \right)_{,r} \right]_{,r} = 0. \end{aligned} \tag{7}$$

The quoted form given by equation (7), where we excluded the derivatives, is particularly easy to integrate. The fundamental system is given by

$$u_r = A\, r + \frac{B}{r^2}, \tag{8}$$

where A and B are constants which can be fixed by the stress boundary conditions

$$\begin{aligned} \sigma_{rr}(r_i) &= -p_i\ , \\ \sigma_{rr}(r_a) &= -p_a\ , \end{aligned} \tag{9}$$

leading to the well-known text-book solution, cf. e.g. [19]

$$\sigma_{rr} = \frac{p_i r_i^3 - p_a r_a^3}{r_a^3 - r_i^3} - (p_i - p_a)\, \frac{r_a^3 \cdot r_i^3}{r_a^3 - r_i^3} \cdot \frac{1}{r^3}, \tag{10}$$

$$\left.\begin{matrix} \sigma_{\varphi\varphi} \\ \sigma_{\vartheta\vartheta} \end{matrix}\right\} = \frac{p_i r_i^3 - p_a r_a^3}{r_a^3 - r_i^3} + (p_i - p_a)\, \frac{r_a^3 \cdot r_i^3}{2\left(r_a^3 - r_i^3\right)} \cdot \frac{1}{r^3}, \tag{11}$$

$$u_r = \frac{r}{2G} \left[\frac{1-2\nu}{1+\nu} \cdot \frac{p_i r_i^3 - p_a r_a^3}{r_a^3 - r_i^3} + (p_i - p_a)\, \frac{r_a^3 r_i^3}{2\left(r_a^3 - r_i^3\right)} \cdot \frac{1}{r^3} \right]. \tag{12}$$

3. Visualization of the stress distribution

Our aim is to provide a representation of the stress state in graphical form by only two diagrams. To this extent, we split the general loading case into two separate parts. For internal pressure only, i.e. $p_a = 0$ and $p_i > 0$, we find for the non-dimensionalized stresses

$$\frac{\sigma_{rr}}{p_i} = \frac{1}{r_a^3 - r_i^3}\left(r_i^3 - \frac{r_a^3 r_i^3}{r^3}\right),$$
$$\frac{\sigma_{\varphi\varphi}}{p_i} = \frac{\sigma_{\vartheta\vartheta}}{p_i} = \frac{1}{r_a^3 - r_i^3}\left(r_i^3 + \frac{1}{2}\frac{r_a^3 r_i^3}{r^3}\right).$$

On the other hand, for external pressure only, i.e. $p_i = 0$ and $p_a > 0$, we have

$$\frac{\sigma_{rr}}{p_a} = \frac{1}{r_a^3 - r_i^3}\left(-r_a^3 + \frac{r_a^3 r_i^3}{r^3}\right),$$
$$\frac{\sigma_{\varphi\varphi}}{p_a} = \frac{\sigma_{\vartheta\vartheta}}{p_a} = \frac{1}{r_a^3 - r_i^3}\left(-r_a^3 - \frac{1}{2}\frac{r_a^3 r_i^3}{r^3}\right).$$

By addition of the non-dimensionalized stresses, we see immediately

$$\frac{\sigma_{rr}}{p_i} + \frac{\sigma_{rr}}{p_a} = \frac{\sigma_{\varphi\varphi}}{p_i} + \frac{\sigma_{\varphi\varphi}}{p_a} = \frac{\sigma_{\vartheta\vartheta}}{p_i} + \frac{\sigma_{\vartheta\vartheta}}{p_a} = -1. \tag{13}$$

Therefore, the stress distributions for the load case of outer pressure are obtained by a mere shift of the values of the ordinate axis of the stress distributions for the inner pressure load case. To the best of the authors knowledge, confirmed by an intensive literature search, this fact has been overlooked by researches and text-book authors in the field, even by Love [32].

In addition, we introduce the dimensionless thickness parameter

$$\kappa := \frac{r_a}{r_i}, \quad \kappa > 1$$

(the greater the value of κ, the thicker is the vessel), and the dimensionless radial coordinate

$$s := \frac{r - r_i}{r_a - r_i}.$$

In this way, the radial domain $r_i \le r \le r_a$ is mapped onto the domain $0 \le s \le 1$, with $s = 0$ corresponding to the inner boundary $r = r_i$ and $s = 1$ corresponding to the outer boundary $r = r_a$. Thus, the dimensionless stress distributions are given by

$$\frac{\sigma_{rr}}{p_i} = -\frac{\sigma_{rr}}{p_a} - 1 = \frac{1}{\kappa^3 - 1}\left(1 - \frac{\kappa^3}{[(\kappa - 1)s + 1]^3}\right),$$
$$\frac{\sigma_{\varphi\varphi}}{p_i} = \frac{\sigma_{\vartheta\vartheta}}{p_i} = -\frac{\sigma_{\varphi\varphi}}{p_a} - 1 = -\frac{\sigma_{\vartheta\vartheta}}{p_a} - 1 = \frac{1}{\kappa^3 - 1}\left(1 + \frac{1}{2}\frac{\kappa^3}{[(\kappa - 1)s + 1]^3}\right),$$

which are plotted in Figure 2. Of course, the general load case of combined inner and outer pressure is given by the superposition of the two special cases. Therefore, the stress state in any point of the vessel can be obtained graphically from Figure 2 alone.

4. Dimensioning of thick-walled spherical vessels via maximum stresses

For the technically most important case of only inner pressure, the radial stress has its maximum absolute value at the inner radius where it equals p_i. The parameter κ defines the speed of decaying towards the outer radius.

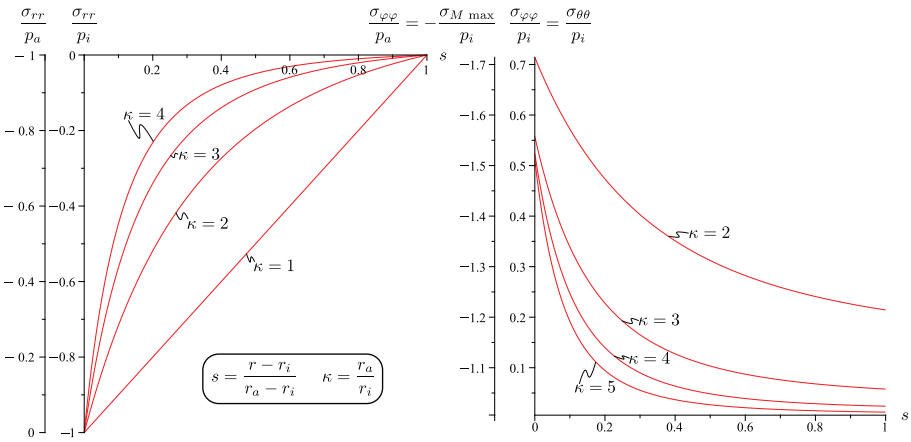

Figure 2. Stress distribution in a thick-walled pressure vessel loaded by inner pressure p_i (right hand ordinates) and outer pressure p_a (left hand ordinates).

The hoop stress has its maximum absolute value at the inner radius, too. For thick vessels $\kappa \to \infty$ the hoop stress maximum absolute value converges fast towards $p_i/2$, whereas it is unbounded for $\kappa \to 1$, i.e. for thin vessels. This means on the one hand that for very thick vessels the absolute maximum component of stress is indeed the applied inner pressure, which makes the thick-walled sphere an optimal pressure vessel in that sense. On the other hand, the hoop stress will be the absolute maximum stress for all technically relevant vessels which are only moderately thick, which is quantified below.

The maximum hoop stresses can be derived by insertion of $s = 0$ into the stress distribution which delivers a simple formula

$$\frac{\sigma_{\varphi\varphi\,\max}}{p_i} = \frac{\sigma_{\vartheta\vartheta\,\max}}{p_i} = \frac{\kappa^3 + 2}{2(\kappa^3 - 1)}. \tag{14}$$

These stresses are the absolute maximum component of stress if they exceed 1, what happens for all $\kappa < \sqrt[3]{4} \approx 1.59$. If $\kappa \geq \sqrt[3]{4}$ the absolute maximum component of stress is the applied pressure p_i. However, of course, $\kappa \geq \sqrt[3]{4}$ is a case that has only restricted technical relevance.

Since the maximum hoop stress is like already mentioned unbounded for $\kappa \to 1$, the radial stresses will be negligible for the dimensioning of sufficiently thin vessels. Having an exact solution, we are able to quantify how thin a vessel has to be so that it can be designed by the maximum stress.

By international standards and directives like, e.g. the pressure equipment directive (2014/68/EU formerly 97/23/EC) of the EU, cf. [33], or the ISO-standard for refillable seamless steel gas cylinders, cf. [34], a steel used for pressure vessels has to be sufficiently ductile which is quantified by a minimum strain to rupture of 14%. (Obviously, the case of brittle rapture is much more dangerous.) Therefore, the most accurate assumption is that the maximum allowable stress is limited by the von Mises yield criterion. In our case, the dimensionless von Mises stress is simply given by

$$\frac{\sigma_M}{p_i}(s) = \frac{\sigma_{\varphi\varphi}}{p_i}(s) - \frac{\sigma_{rr}}{p_i}(s)$$

and equals the dimensionless Tresca yield stress, which is also used for the dimensioning of pressure vessels, cf. [35]. The overall maximum von Mises stress is obviously located at the inner radius ($s = 0$) and has the value

$$\frac{\sigma_{M\,\max}}{p_i} = -\frac{\sigma_{\varphi\varphi}}{p_a}(s = 0) = 1 + \frac{\sigma_{\varphi\varphi\,\max}}{p_i}.$$

Therefore, the overall maximum von Mises stress can be read off the left hand ordinate of the right diagram in Figure 2 by changing the sign or it can be derived by adding 1 to equation (14). The absolute error Δ for taking the hoop stress as comparison stress is obviously p_i. The relative error increases quite fast as illustrated in Figure 3.

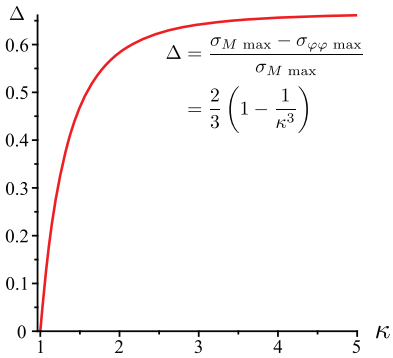

Figure 3. Relative error by using the hoop stress for dimensioning rather than the overall maximum von Mises stress.

1% relative error is not achieved before $\kappa < 1.0051$, i.e. before the thickness t is less than $0.0051\, r_i$. 5% relative error is not achieved before $\kappa < 1.0263$. Given these numbers it seems unavoidable to use a yield criterion for a safe design of pressure vessels in the technically important regime, which is done by the technical standards cited above.

For the load case of only outer pressure p_a the maximum absolute value of radial stress is also p_a. For very thick-walled vessels $\kappa \to \infty$ the absolute maximum value of the dimensionless hoop stresses converges to the notch factor $3/2$ of a spherical inclusion in an infinite continuum under tensile stress.

For the combined load case, the radial stress stays bounded in any case, whereas, the hoop stresses are maximal for the case that p_a and p_i have opposing signs, e.g. internal pressure and external tension, so that it is kind of natural to use $p_i - p_a$ as a quotient for dimensioning formulas. For the maximum hoop stress at the inner radius we obtain a correction to equation (14) for applied outer pressure

$$\frac{\sigma_{\varphi\varphi\,\max}}{p_i - p_a} = \frac{\sigma_{\vartheta\vartheta\,\max}}{p_i - p_a} = \frac{\kappa^3 + 2}{2(\kappa^3 - 1)} - \frac{p_a}{p_i - p_a}. \tag{15}$$

If we add the inner pressure divided by $p_i - p_a$ to the right hand side of the formula, the same formula for the absolute maximum von Mises stress is recovered, i.e. the right hand side of equation (14) + 1, only the quotient on the left hand side changes to $p_i - p_a$.

5. Dimensioning of thin-walled spherical vessels loaded by inner pressure

All stresses take their maximum absolute values at the inner radius as we have seen before, therefore, one can derive approximative formulas for the dimensioning of thin-walled vessels for the load case of only inner pressure by evaluating the stresses at $r = r_i$, while setting $r_a := r_i + t$, where $0 < \frac{t}{r_i} \ll 1$. In this way we obtain fractions of polynomials in t which lead to the approximative formulas if we take only the dominant terms for $t \to 0$ into account, i.e. the ones with the lowest power of t. Indeed, we obtain

$$\begin{aligned}
\sigma_{rr} &= \frac{p_i r_i^3}{3r_i^2 t + 3r_i t^2 + t^3}\left[1 - 1 - 3\frac{t}{r_i} - 3\frac{t^2}{r_i^2} - \frac{t^3}{r_i^3}\right] \\
&\approx -\frac{3p_i r_i^2 t}{3r_i^2 t} = -p_i, \\
\sigma_{\varphi\varphi} = \sigma_{\vartheta\vartheta} &= \frac{p_i r_i^3}{3r_i^2 t + 3r_i t^2 + t^3}\left[1 + \frac{1}{2}\left(1 + 3\frac{t}{r_i} + 3\frac{t^2}{r_i^2} + \frac{t^3}{r_i^3}\right)\right], \\
\sigma_{\varphi\varphi} = \sigma_{\vartheta\vartheta} &\approx \frac{\frac{3}{2}p_i r_i^3}{3r_i^2 t} = \frac{p_i r_i}{2t},
\end{aligned} \tag{16}$$

where equation (16) equals the classical equation (1) for thin-walled pressure vessels. The formula is, like in the exact case, the one which is dominant for the dimensioning of structures since it is unbound for $t \to 0$ in

contrast to the radial stress. (That is also the reason why these formulas cannot be derived by evaluating the limit value for $t \to 0$.)

The classical equation (16) is an approximation of the exact equation (14) for sufficiently thin-walled vessels

$$\frac{\sigma^{(16)}_{\varphi\varphi\ \mathrm{Kessel}}}{p_i} = \frac{\sigma^{(16)}_{\vartheta\vartheta\ \mathrm{Kessel}}}{p_i} = \frac{r_i}{2t} = \frac{1}{2(\kappa - 1)}. \tag{17}$$

Having its exact counterpart, we can answer questions concerning the quality of this approximation; e.g. we can compute an explicit formula for the absolute error in the dimensionless hoop stress

$$\left| \frac{\sigma_{\varphi\varphi\ \max}}{p_i} - \frac{\sigma^{(16)}_{\varphi\varphi\ \mathrm{Kessel}}}{p_i} \right| = \frac{1}{2} \frac{\kappa^2 - 1}{\kappa^2 + \kappa + 1} < \varepsilon.$$

For deriving a necessary ratio κ in order to achieve a certain accuracy ε, we obtain a simple formula, if we solve the inequality above for κ

$$\kappa < \frac{1}{1 - 2\varepsilon} \left(\varepsilon + \sqrt{1 - 3\varepsilon^2} \right)$$

and linearize it for small errors $\varepsilon \ll 1$

$$\kappa < 1 + 3\varepsilon.$$

E.g. the error is below 0.01, if $\kappa < 1.03$.

6. Cylindrical vessel

In an analog manner it is possible to investigate the problem of a cylindrical pressure vessel with infinite length in the z-direction with an associated cylindrical (r, φ, z)-coordinate system.

Again, due to the symmetry, the displacement takes place in radial direction only

$$u_r = u_r(r),\ u_\varphi = 0,\ u_z = 0.$$

so that we have only two non-vanishing components of the linearized strain tensor, which are

$$\varepsilon_{rr} = u_{r,r} \text{ and } \varepsilon_{\varphi\varphi} = \frac{u_r}{r}.$$

The solution is limited to the (hypothetical) case that the longitudinal displacement is set to zero for $z \to \pm\infty$, i.e. plane strain conditions are assumed. The more realistic situation for pressure vessels with closed ends will be merely communicated below.

In contrast, all diagonal elements of the stress tensor are non-vanishing and follow by insertion into Hooke's law. The only non-trivial equilibrium equation is the one in the radial direction

$$\sigma_{rr,r} + \frac{1}{r} \left(\sigma_{rr} - \sigma_{\varphi\varphi} \right) = 0,$$

which leads to the ordinary differential equation

$$\left(\frac{1}{r} (r\, u_r)_{,r} \right)_{,r} = 0$$

with fundamental solution

$$u_r = A\, r + \frac{1}{r} B.$$

The constants A and B can be derived from the boundary conditions given by equation (9), which in turn leads to the stress distribution

$$\sigma_{rr} = \frac{p_i r_i^2 - p_a r_a^2}{r_a^2 - r_i^2} + \frac{p_a - p_i}{r_a^2 - r_i^2}\frac{r_i^2 r_a^2}{r^2}, \tag{18}$$

$$\sigma_{\varphi\varphi} = \frac{p_i r_i^2 - p_a r_a^2}{r_a^2 - r_i^2} - \frac{p_a - p_i}{r_a^2 - r_i^2}\frac{r_i^2 r_a^2}{r^2}, \tag{19}$$

$$\sigma_{zz} = 2\nu\,\frac{p_i r_i^2 - p_a r_a^2}{r_a^2 - r_i^2} = \text{ const.} \tag{20}$$

For cylinders with closed ends, the prefactor 2ν in the equation for σ_{zz} has to be merely replaced by 1.

Splitting the loading cases again delivers on the one hand for the case of internal pressure, i.e. $p_i > 0$ and $p_a = 0$

$$\frac{\sigma_{rr}}{p_i} = \frac{1}{r_a^2 - r_i^2}\left(r_i^2 - \frac{r_a^2 r_i^2}{r^2}\right),$$
$$\frac{\sigma_{\varphi\varphi}}{p_i} = \frac{1}{r_a^2 - r_i^2}\left(r_i^2 + \frac{r_a^2 r_i^2}{r^2}\right),$$
$$\frac{\sigma_{zz}}{2\nu p_i} = \frac{r_i^2}{r_a^2 - r_i^2},$$

and on the other hand, for the loading case of external pressure only, i.e., $p_i = 0$ and $p_a > 0$,

$$\frac{\sigma_{rr}}{p_a} = \frac{1}{r_a^2 - r_i^2}\left(-r_a^2 + \frac{r_a^2 r_i^2}{r^2}\right),$$
$$\frac{\sigma_{\varphi\varphi}}{p_a} = \frac{1}{r_a^2 - r_i^2}\left(-r_a^2 - \frac{r_a^2 r_i^2}{r^2}\right),$$
$$\frac{\sigma_{zz}}{2\nu p_a} = -\frac{r_a^2}{r_a^2 - r_i^2}.$$

Again, by addition, we find immediately

$$\frac{\sigma_{rr}}{p_i} + \frac{\sigma_{rr}}{p_a} = \frac{\sigma_{\varphi\varphi}}{p_i} + \frac{\sigma_{\varphi\varphi}}{p_a} = \frac{\sigma_{zz}}{2\,\nu\,p_i} + \frac{\sigma_{zz}}{2\,\nu\,p_a} = -1. \tag{21}$$

Introducing the dimensionless thickness parameter κ and the dimensionless radial coordinate s, we find

$$\frac{\sigma_{rr}}{p_i} = -\frac{\sigma_{rr}}{p_a} - 1 = \frac{1}{\kappa^2 - 1}\left(1 - \frac{\kappa^2}{[(\kappa - 1)s + 1]^2}\right),$$
$$\frac{\sigma_{\varphi\varphi}}{p_i} = -\frac{\sigma_{\varphi\varphi}}{p_a} - 1 = \frac{1}{\kappa^2 - 1}\left(1 + \frac{\kappa^2}{[(\kappa - 1)s + 1]^2}\right),$$
$$\frac{\sigma_{zz}}{2\,\nu\,p_i} = -\frac{\sigma_{zz}}{2\,\nu\,p_a} - 1 = \frac{1}{\kappa^2 - 1}.$$

Therefore, the same argument applies that the graphical representation of the stresses at any point in the vessel may be given by merely two diagrams, which are depicted in Figure 4.

For the technically most important load case of only inner pressure the maximum hoop stress is

$$\frac{\sigma_{\varphi\varphi\ \max}}{p_i} = \frac{1 + \kappa^2}{\kappa^2 - 1}, \tag{22}$$

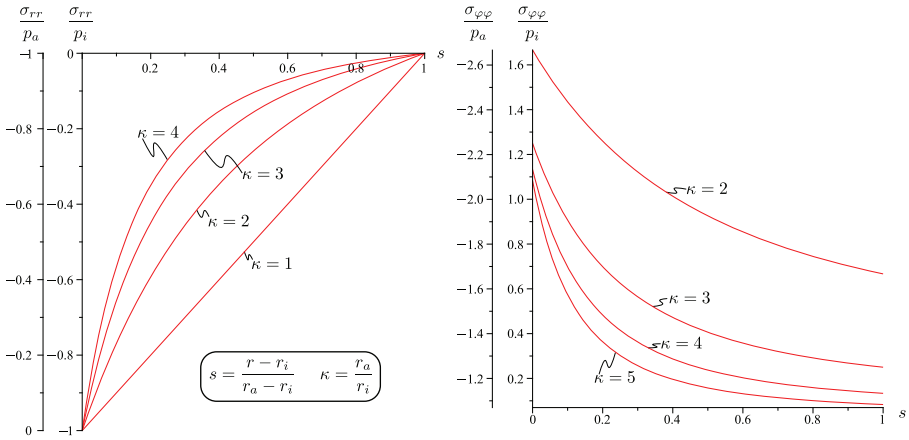

Figure 4. Stress distribution in a thick-walled cylindrical pressure vessel loaded by inner pressure p_i (right hand ordinates) and outer pressure p_a (left hand ordinates).

and is located at the inner radius ($s = 0$), again, which also holds true for the von Mises stress which maximum value is given by

$$\frac{\sigma_{M\,\max}}{p_i} = \sqrt{\frac{(1-2\nu)^2 + 3\kappa^4}{(\kappa^2-1)^2}}, \tag{23}$$

for the plane strain case, whereas, for closed-end vessels, we find

$$\frac{\sigma_{M\,\max}}{p_i} = \sqrt{3}\frac{\kappa^2}{\kappa^2-1}. \tag{24}$$

The approximation formula for the maximum hoop stress given by equation (22) for thin vessels is the classical equation (1)

$$\frac{\sigma_{\varphi\varphi\,\max}}{p_i} \approx \frac{r_i}{t} = \frac{1}{\kappa-1}. \tag{25}$$

Note that some ASTM international (formerly known as American Society for Testing and Materials) standards, e.g. [36–38], which treat the testing (and not the design) of pressure vessels, use a more conservative estimate for the hoop stress which is obtained by adding $1/2$ to the right hand side of equation (25). By simply inserting the approximation given by equation (25), the maximum Tresca yield stress is given by

$$\frac{\sigma_{T\,\max}}{p_i} = \frac{r_i}{t} + 1 = \frac{\kappa}{\kappa-1}.$$

Solving the formula for the required thickness t leads to the formula

$$t = \frac{p_i D_a}{2\sigma_T},$$

where D_a is the outer diameter $D_a = 2r_i + 2t$, which is used in DIN 2413, cf. [35], for the dimensioning of pipes, if we set the safety to $S = 1$ (i.e. no safety) for the purpose of comparison. Without safety, the standard is only a conservative estimate for the comparison stress σ_V in the domain $1 < \kappa < 1/(\sqrt{3}-1) \approx 1.367$, although the standard is specified for all $\kappa < 2$. This is resolved by applying the minimum safety of $S = 1.4$ which is depicted in Figure 5.

From a mechanical point of view, this is an interesting result since the Tresca hypothesis is known to be conservative in general. Indeed, if we linearize the yield stress formulas we obtain

$$\frac{\sigma_{M\,\max}}{p_i} = \sqrt{3}\,\frac{\kappa^2}{\kappa^2-1} \approx \frac{1}{2}\sqrt{3}\,\frac{r_i}{t} + \frac{3}{4}\sqrt{3} = \frac{1}{2}\sqrt{3}\,\frac{1}{\kappa-1} + \frac{3}{4}\sqrt{3}$$

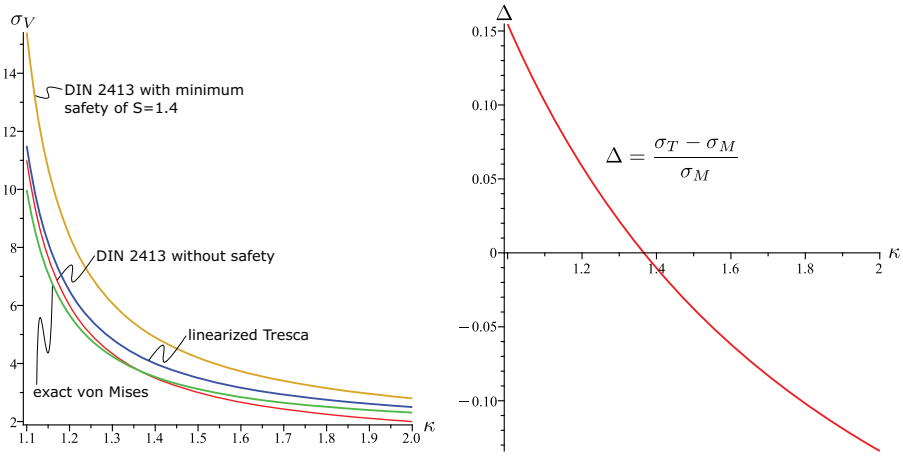

Figure 5. On the left: Comparison stresses σ_V associated with DIN 2413 in comparison to the absolute maximum von Mises stress of the exact solution (24) and the linearized Tresca yield stress (26). On the right: Relative error of the DIN 2413 comparison stress without safety ($S = 1$).

for the von Mises stress for closed-end vessels, cf. equation (24), and

$$\frac{\sigma_{T\,\max}}{p_i} = 2\,\frac{\kappa^2}{\kappa^2 - 1} \approx \frac{r_i}{t} + \frac{3}{2} = \frac{1}{\kappa - 1} + \frac{3}{2} \tag{26}$$

for the Tresca yield stress. Obviously, the exact Tresca yield stress is in general greater than the von Mises stress. The linearization of the Tresca stress is, furthermore, conservative in a larger domain, precisely until $\kappa = 2 + \sqrt{3} \approx 3.73$ and henceforth conservative in the whole domain for which the DIN 2413 is specified, i.e. $\kappa < 2$, as depicted in Figure 5. This may serve as a reminder that the linearization should always be the last step. However, the relative error between the exact von Mises stress and the norm estimate for safety $S = 1$ is smaller than it would be, if the linearized Tresca stress given by equation (26) would be used. The error between the DIN 2413 for safety $S = 1$ and the exact von Mises solution given by equation (24) may be up to 15% as depicted in the right diagram of Figure 5.

7. Conclusions

In this contribution we presented a novel and easy way to construct the stress state in arbitrary points in thick-walled pressure vessels graphically from only two diagrams, cf. Figures 2 and 4. The representation is based on a simple connection between the inner-pressure and outer-pressure solution, cf. equations (13) and (21), which has not been discovered before to our best knowledge. It is astonishing that it is still possible to reveal new aspects of such a rather classical problem.

Funding

The author(s) received no financial support for the research, authorship, and/or publication of this article.

References

[1] Lamé, G. *Leçons Sur la Théorie Mathématique de l'Élasticité des Corps Solides*. Paris, France: Bachelier, 1852.
[2] Sinclair, G, and Helms, J. A review of simple formulae for elastic hoop stresses in cylindrical and spherical pressure vessels: What can be used when. *Int J Pres Ves Pip* 2015; 128: 1–7.
[3] Bürgel, R. *Festigkeitslehre und Werkstoffmechanik: Lehr- und Übungsbuch Festigkeitslehre*. Wiesbaden: Vieweg+Teubner Verlag, 2005.
[4] Gere, J, and Timoshenko, S. *Mechanics of Materials*. 3rd ed. London: Chapman & Hall, 1991.
[5] Gere, JM. *Mechanics of Materials*. 5th SI ed. Cheltenham: Nelson Thornes, 2002.
[6] Lardner, TJ, and Archer, RR. *Mechanics of Solids: An Introduction*. 2nd ed. New York: McGraw-Hill, 1994.

[7] Richard, H, and Sander, M. *Technische Mechanik - Festigkeitslehre: Lehrbuch mit Praxisbeispielen, Klausuraufgaben und Lösungen*. 1st ed. Wiesbaden: Friedr. Vieweg & Sohn Verlag / GWV Fachverlage GmbH, 2006.

[8] Hibbeler, RC. *Engineering Mechanics*. 4th ed. Prentice Hall, 2000.

[9] Balke, H. *Einführung in die Technische Mechanik: Festigkeitslehre*. 3rd ed. Berlin: Springer, 2014.

[10] Budynas, RG. *Advanced Strength and Applied Stress Analysis*. 2nd ed. New York: McGraw-Hill, 1977.

[11] Dankert, J, and Dankert, H. *Technische Mechanik: Statik, Festigkeitslehre, Kinematik/Kinetik*. 7th ed. Wiesbaden: Springer Fachmedien Wiesbaden, 2013.

[12] Hahn, HG. *Elastizitätstheorie: Grundlagen der linearen Theorie und Anwendungen auf eindimensionale, ebene und räumliche Probleme*. 1st ed. Stuttgart: Teubner, 1985.

[13] Hibbeler, R. *Technische Mechanik. 2. Festigkeitslehre: Lehr-und Übungsbuch*. 6th ed. München: Pearson, 2006.

[14] Altenbach, H. *Holzmann/Meyer/Schumpich Technische Mechanik Festigkeitslehre*. 11th ed. Wiesbaden: Springer Vieweg, 2014.

[15] Kachanov, M, Shafiro, B, and Tsukrov, I. *Handbook of Elasticity Solutions*. 1st ed. Dordrecht: Springer Netherlands, 2003.

[16] Läpple, V. *Einführung in die Festigkeitslehre: Lehr- und Übungsbuch*. 3rd ed. Wiesbaden: Vieweg+Teubner Verlag, 2012.

[17] Mang, HA, and Hofstetter, G. *Festigkeitslehre*. 4th ed. Berlin, Heidelberg: Springer, 2013.

[18] Riley, WF, Sturges, LD, and Morris, DH. *Mechanics of Materials*. 6th ed. New York: Wiley, 1999.

[19] Stark, R. *Festigkeitslehre: Aufgaben und Lösungen*. Heidelberg: Physica-Verlag, 2006.

[20] Timoshenko, SP, and Goodier, JN. *Theory of Elasticity*. 3rd ed. New York: McGraw Hill, 1970.

[21] Wittenburg, J, and Pestel, E. *Festigkeitslehre: Ein Lehr- und Arbeitsbuch*. 3rd ed. Berlin: Springer, 2001.

[22] Bland, DR. Elastoplastic thick-walled tubes of work-hardening material subject to internal and external pressures and to temperature gradients. *J Mech Phys Solids* 1956; 4(4): 209–229.

[23] Gao, XL, and Park, S. Variational formulation of a simplified strain gradient elasticity theory and its application to a pressurized thick-walled cylinder problem. *Int J Solids Struct* 2007; 44(22-23): 7486–7499.

[24] Gao, XL, Park, S, and Ma, H. Analytical solution for a pressurized thick-walled spherical shell based on a simplified strain gradient elasticity theory. *Mathematics and Mechanics of Solids* 2009; 14(8): 747–758.

[25] Naumenko, K, and Altenbach, H. *Modeling of creep for structural analysis*. Berlin: Springer-Verlag, 2007.

[26] Naumenko, K, and Altenbach, H. *Modeling High Temperature Materials Behavior for Structural Analysis, Part I: Continuum Mechanics Foundations and Constitutive Models*, *Advanced Structured Materials*, vol. 28. Switzerland: Springer International Publishing, 2016.

[27] Atashipour, SA, Sburlati, R, and Atashipour, SR. Elastic analysis of thick-walled pressurized spherical vessels coated with functionally graded materials. *Meccanica* 2014; 49(12): 2965–2978.

[28] Bayat, Y, Ghannad, M, and Torabi, H. Analytical and numerical analysis for the FGM thick sphere under combined pressure and temperature loading. *Arch Appl Mech* 2012; 82(2): 229–242.

[29] Tutuncu, N, and Ozturk, M. Exact solutions for stresses in functionally graded pressure vessels. *Compos Part B: Eng* 2001; 32(8): 683–686.

[30] Tutuncu, N and Temel, B. A novel approach to stress analysis of pressurized FGM cylinders, disks and spheres. *Compos Struct* 2009; 91(3): 385–390.

[31] Lim, T. *Auxetic Materials and Structures*. Singapore: Springer Science + Business Media, 2015.

[32] Love, AEH. *Treatise on the Mathematical Theory of Elasticity*. New York: Dover Publications, 1944.

[33] Verband der TÜV e.V. (ed.), *AD 2000-Regelwerk*. Berlin: Beuth Verlag, 2014.

[34] DIN EN ISO 9809-1:2010-10. Gas cylinders - refillable seamless steel gas cylinders - design, construction and testing - part 1: Quenched and tempered steel cylinders with tensile strength less than 1100 MPa. DIN EN ISO 9809-1, 2010.

[35] DIN 2413:2011-06. Seamless steel tubes for oil - and water-hydraulic systems - calculation rules for pipes and elbows for dynamic loads. DIN 2413, 2011.

[36] ASTM Standard D1598-15a. Standard test method for time-to-failure of plastic pipe under constant internal pressure. ASTM International, West Conshohocken, PA, 2015.

[37] ASTM Standard D1599-14. Standard test method for resistance to short-time hydraulic pressure of plastic pipe, tubing, and fittings. ASTM International, West Conshohocken, PA, 2014.

[38] ASTM Standard D2992-12. Standard practice for obtaining hydrostatic or pressure design basis for “fiberglass” (glass-fiber-reinforced thermosetting-resin) pipe and fittings. ASTM International, West Conshohocken, PA, 2012.